Author/s:
Molloy, CP;Yao, Y;Kammoun, H;Bonnard, T;Hoefer, T;Alt, K;Tovar-Lopez, F;Rosengarten, G;Ramsland, PA;van der Meer, AD;van den Berg, A;Murphy, AJ;Hagemeyer, CE;Peter, K;Westein, E

Title:
Shear-sensitive nanocapsule drug release for site-specific inhibition of occlusive thrombus formation

Date:
2017-05-01

Citation:
Molloy, C. P., Yao, Y., Kammoun, H., Bonnard, T., Hoefer, T., Alt, K., Tovar-Lopez, F., Rosengarten, G., Ramsland, P. A., van der Meer, A. D., van den Berg, A., Murphy, A. J., Hagemeyer, C. E., Peter, K. & Westein, E. (2017). Shear-sensitive nanocapsule drug release for site-specific inhibition of occlusive thrombus formation. Journal of Thrombosis and Haemostasis, 15 (5), pp.972-982. https://doi.org/10.1111/jth.13666.

Received Date : 14-Jul-2016
Revised Date : 24-Jan-2017
Accepted Date : 20-Feb-2017
Article type : Original Article - Platelets

Shear sensitive nanocapsule drug release for site specific inhibition of occlusive thrombus formation

Short title: Site specific inhibition of thrombosis

Christopher P. Molloy[*], Yu Yao[*], Helene Kammoun[†], Thomas Bonnard[‡], Thomas Hoefer[*], Karen Alt[‡], Francisco Tovar-Lopez[§], Gary Rosengarten[§], Paul A. Ramsland[**], Andries D. van der Meer[††], Albert van den Berg[††], Andrew J. Murphy[†], Christoph E. Hagemeyer[‡], Karlheinz Peter[*,‡‡], Erik Westein[*].

[*]*Atherothrombosis and Vascular Biology, Baker IDI Heart and Diabetes Institute. 75 Commercial rd, Melbourne VIC 3004, Australia.* [†]*Haematopoiesis and Leukocyte Biology, Baker IDI Heart & Diabetes Institute, Melbourne, Victoria, 3004, Australia.* [‡]*Nano Biotechnology Laboratory, Australian Centre for blood diseases, Monash University, Melbourne, Victoria, 3004, Australia.* [§]*School of Engineering, RMIT University, 376 Swanston Street, Melbourne VIC 3000, Australia.* [**]*School of Science, RMIT University, Bundoora, Australia; Centre for Biomedical Research, Burnet Institute, Melbourne, Australia*; *Department of Immunology, Monash University, Melbourne, Australia; Department of Surgery at Austin Health, University of Melbourne, Heidelberg, Australia.* [††]*MIRA Institute for Biomedical Technology and Technical Medicine, University of Twente, P.O. Box 217, 7500 AE Enschede, The Netherlands.*

[‡‡]corresponding author; Email: Karlheinz.Peter@bakeridi.edu.au,

Keywords

Antiplatelet drugs; Platelets; Nanocapsules; Drug Delivery Systems; Microfluidics

Word count

Abstract: 199 words / Body: 3996 / figure legends: 1180 / references: 1093

Essentials

- Vessel stenosis due to large thrombus formation increases local shear 1-2 orders of magnitude.
- High shear at stenotic sites was exploited to trigger eptifibatide release from nanocapsules.
- Local delivery of eptifibatide prevented vessel occlusion without increased tail bleeding times.
- Local nanocapsule delivery of eptifibatide may be safer than systemic anti-platelet therapies.

Abstract

Background. Myocardial infarction and stroke remain the leading causes of mortality and morbidity. The major limitation of current antiplatelet therapy is that their effective concentrations are limited due to bleeding complications. Targeted delivery of antiplatelet drug to sites of thrombosis would overcome these limitations.

Objectives. Here, we have exploited a key biomechanical feature specific to thrombosis; significantly increased blood shear stress due to a reduction in the lumen of the vessel, to achieve site directed delivery of the clinically used antiplatelet agent eptifibatide using shear-sensitive phosphatidylcholine based nanocapsules.

Methods. $2.8x10^{12}$ PC based nanocapsules with high dose encapsulated eptifibatide were introduced in microfluidic blood perfusion assays and in *in vivo* models of thrombosis and tail bleeding.

Results. Shear-triggered nanocapsule delivery of eptifibatide inhibited *in vitro* thrombus formation selectively under stenotic and high shear flow conditions above 1,000 s^{-1} shear rate while leaving thrombus formation under physiological shear rates unaffected. Thrombosis was effectively prevented in *in vivo* models of vessel wall damage. Importantly, mice infused with shear sensitive antiplatelet nanocapsules did not display prolonged bleeding times.

Conclusions. Targeted delivery of eptifibatide by shear-sensitive nanocapsules offers site specific antiplatelet potential and may form a basis for developing more potent and safer antiplatelet drugs.

Introduction

Superimposed thrombus formation at sites of atherosclerosis restricts the remaining lumen and increases local blood shear stresses to extreme values. Recent studies demonstrated that arterial thrombosis and vascular remodelling are strongly promoted by biomechanical forces, particularly pathological shear stress [1]. In addition, we and others previously demonstrated that von Willebrand factor unfolding or activation [2, 3] and shear gradient dependent platelet aggregation mechanisms [4] promote arterial thrombosis. Large thrombi create a local microenvironment with high shear stress which exacerbates thrombus growth. Current antiplatelet therapy is not tailored to respond to local prothrombotic effects of pathological shear stress [5]. Furthermore, the systemic nature of antiplatelet therapy results in only limited drug concentrations at sites of thrombus formation yet is directly associated with an increased bleeding risk, including fatal bleedings.

Various targeting strategies have been explored to increase local drug concentration at sites of thrombi. Recent studies have elegantly demonstrated the potential of targeting the fibrinolytic agent tPA to blood clots by using GPIIb/IIIa activation-specific single-chain antibodies [6-8] or shear sensitive co-polymers of lactic acid and glycolic acid which act as a drug carrier that disaggregates at high shear stress to allow local binding to developed thrombi [9]. Therapeutics involving nanocapsules have shown enormous promise for targeted delivery of drugs at disease sites, partly because of their high payload of drugs and the capability to functionalize their surface with adhesive ligands [10]. However, to date, the use of therapeutic nanocapsules in the prevention or treatment of thrombosis or vascular remodelling has been limited [9]. One of the main reasons for the lack of translation of nanocapsules to the clinic is that there are few platforms that can rapidly evaluate the biological behaviour of antithrombotic nanocapsules under *in vitro* conditions that can be correlated with their performance *in vivo* [11]. Traditional methods to evaluate release of encapsulated contents from lipid nanocapsules typically involve measurements of spectroscopic changes of the bulk sample when encapsulated compounds react with the external medium. These methods, although useful to evaluate stressors on nanocapsule stability and latency, are not functional assays that allow assessment of local drug release at desired locations such as sites of thrombus formation.

We developed microfluidic platelet function assays and employed animal thrombosis models to directly determine phosphatidylcholine based nanocapsule delivery of the antiplatelet drug eptifibatide specifically at vessel segments harbouring pathophysiological shear stress. Drug release and shear sensitivity of the nanocapsules could be controlled and was measured by the degree of platelet aggregation inhibition. Localization of high concentrations of antiplatelet

drugs to areas of high shear stress demonstrated effective antiplatelet action without prolonging tail bleeding times. This study demonstrates the feasibility and potential application of nanocapsule antiplatelet drug delivery to sites of thrombosis.

Methods

Nanocapsule preparation. Nanocapsules were prepared from phosphatidylcholine (PC) (Avanti;840051C) supplemented where indicated with 0.06mol% ethoxylated fatty alcohol poly(oxyethylene)(10) stearyl ether (Brij76) using the thin-film rehydration method. 16 µmol of lipid in chloroform was added to a flat-bottomed beaker and dried with nitrogen. Samples were left covered in a vacuum desiccator overnight to produce a dried multi lamellar lipid film. Samples were rehydrated with a 1mL phosphate buffered saline (PBS) solution with indicated anti-platelet drugs for 10 minutes at 55°C. Samples were subjected to 6 freeze thaw cycles between liquid nitrogen and a 37°C water bath, to produce Large Unilamellar Vesicles (LUVs). Samples were then extruded 11 times through a polycarbonate membrane with 200 nm pore sizes (Whatman Track-Etch membrane) at 55°C to produce vesicles at ~200 nm diameter, assessed by light scattering using a Zetasizer µV analyser (Malvern, UK). Non-encapsulated drugs were removed by dialysis against PBS.

Microfluidic flow channels and blood perfusion. PDMS channels were manufactured using an SU-8 master mold that was fabricated by standard photolithography methods as previously described [3]. Wall shear rates of the input flow for the microchannels were calculated from volumetric flow rates by using the equation, $\gamma = 6Q/wh^2$. Herein, γ is the wall shear rate (s^{-1}), Q is the volumetric flow rate (mL/sec), w and h is the channel width and height (cm) respectively.

Studies were approved by the local Human Ethics Committee (Alfred Ethics Committee, 118/07). Citrate anticoagulated human whole blood was perfused over a matrix of Horm collagen type I (Takeda, Austria) at indicated coating concentrations and at input shear rates of 500 – 3,000 s^{-1}. Platelets were stained with 0.5 µg/mL DiOC6. Fluorescent nanocapsules were made by incorporation of 0.5 mol% NDB-PE. $1.4x10^{12}$/mL nanocapsules were added to whole blood. Thrombus surface coverage was monitored with wide-field fluorescence microscopy using an Olympus IX81 microscope system.

High speed analysis of nanocapsules in stenosis channels. Nanocapsules loaded with 0.5 µg/mL $DiOC_6$ were perfused at 1,000 s^{-1} through microfluidic channels and imaged at 20,000 frames per second with a Phantom v1610 high-speed camera mounted on an Olympus IX81

microscope. Average particle intensity and size was analysed for 8,000 consecutive frames using ImageJ.

Platelet aggregation. PRP was prepared from sodium citrate (3.2%) anticoagulated whole blood, collected from healthy donors and used within 3 hours. Platelet aggregation was assessed by LTA and induced by ADP in the presence of either PBS, intact- or 'shear disrupted' nanocapsules. Shear disruption of nanocapsules was achieved by vortexing for 3 minutes followed by sonication for 3 min.

***In vivo* thrombosis models.** Approval was obtained from the Alfred Medical Research and Education Precinct Animal Ethics Committee for all experiments involving animals. All mice were anaesthetized by intraperitoneal injection of ketamine/xylazine. Nanocapsules (12.3 mg/ml corresponding to ~$2.8x10^{12}$ nanocapsules/ml) loaded with PBS (PBS-NCs) or eptifibatide (E-NCs) at indicated loading concentrations were infused intravenously as a 100 µL bolus into WT mice 5 minutes or 40 minutes prior to thrombus formation in the carotid artery induced by topical application (3 min) of 5% (w/v) ferric chloride. Occlusive thrombus formation leading to flow cessation in the carotid artery was monitored with a Doppler ultrasound probe (0.5VB; Transonic, Japan). Blood clearance: $2.8x10^{12}$ nanocapsules with 0.5 mol% NDB-PE were injected i.v. and counted in blood samples collected at indicated time points. Counting was performed using fluorescence microscopy in microfluidic channels as liposome density per field of view and normalized against the density at timepoint 0. Organ distribution: After i.v. injection of $2.8x10^{12}$ nanocapsules containing trace amounts of ^{3}H-PC mice were killed after 2 hours. Tissue samples were homogenized in sterile water and ^{3}H radioactivity was determined by liquid scintillation counting. Tissue radioactivity was normalized to sample weight.

Tail bleeding time. The haemostatic potential of mice was assessed by using the template tail bleeding time method. A longitudinal incision, 2 mm deep, 4 mm long, was made starting 10 mm from the proximal side of the tail. Incisions were made over the superficial tail vein running along the left axis of the tail. 100 µL nanocapsule solution was administered i.v. via the tail vein, 5 minutes prior to incision. Tail bleeding was monitored and dabbed with whatman filter paper for up to 20 minutes.

Pulmonary thrombus load model. Thrombi were induced by infusing a mixture of 5% (v/v) Innovin (recombinant tissue factor and synthetic phospholipids) and 10 µg/mL Cy-7 labelled fibrinogen at 5 µL/g body weight (BW) via the tail vein. Mice were sacrificed after 1 hour and perfused with saline. Fibrin(-ogen) content was imaged in excised lungs using an

Odyssey infrared Imager (Li-Cor, USA) and analysed for fluorescence surface area, relative to total lung area using ImageJ software.

Computational fluid dynamics. A finite volume scheme using the OpenFOAM [12] was used to solve numerically the fluid flow equations (Navier–Stokes). The fluid medium was considered homogeneous with a constant density (998 kg/m^3) and Newtonian viscosity as blood can be approximated as a Newtonian fluid at mid and high strain rates. We used the analytical solution of the velocity profile for a Newtonian fluid in rectangular geometries as shown before [13, 14].

Statistical analysis. All data is expressed as mean ± s.e.m. and analysed with one-way ANOVA followed by post hoc Bonferroni's tests unless otherwise indicated. P-values of <0.05 were considered significant.

Results

Site specific delivery of antiplatelet drugs to areas of vessel stenosis.

The haemodynamic environment at sites of vessel stenosis, caused by near occlusive thrombi, is intrinsically prothrombotic due to the generation of high blood shear rates. To test the efficacy of eptifibatide nanocapsules (E-NCs) in specifically inhibiting thrombus formation under stenotic flow conditions we used our microfluidic stenosis model in which thrombus formation is exacerbated in the stenosis apex and outlet zones [3] (Fig. 1a). Perfusion of whole blood in the presence of E-NCs reduced thrombus formation exclusively in the stenotic section (8,000 s^{-1}) whereas it had no effect on thrombus volume in the upstream areas of the channel where shear rates were 1,000 s^{-1} (Fig. 1b,c). These data demonstrate the specificity of the drug delivery towards areas of high shear stress at stenotic vessel segments. This effect of the E-NCs was not due to entrapment of the nanocapsules in the platelet aggregates as no stably adherent fluorescent nanocapsules could be detected (Fig. 1d ii) and all nanocapsules passed the aggregates during blood perfusion (Fig. 1d iii). The overall size distribution of the nanocapsules, measured with dynamic light scattering, did not change after exposure to 10 passes through the stenosis channels at maximum flow rate generating ~40,000 s^{-1} in the stenosis apex (Suppl. Fig. 1).

To estimate the maximal level of eptifibatide release induced by application of shear stress, platelet aggregation was induced by 5 µM ADP in the presence of shear disrupted E-NCs and compared to aggregation levels of PRP incubated with a range of eptifibatide concentrations. Intact E-NCs had minimal inhibitory effect on platelet aggregation, while shear disrupted E-

NCs inhibited platelet aggregation (from 89.7±1.1% to 24.7±8.5%) (Fig. 1e) equivalent to 361 nM free eptifibatide (Fig. 1f). Similar results were obtained for PRP stimulated by 2.5 and 10 µM ADP (Suppl. Fig. 2). Taking into account the original loading concentration of eptifibatide inside the nanocapsules (350 µM), the combined internal volume of 10 µl E-NCs (1.05 µl) and the aggregometry test sample volume (250 µl), the theoretical maximal amount of eptifibatide released by shear stress is 350/(250/1.05)=1.47 µM. However, since the actual released eptifibatide reached 361nM, the release efficiency of eptifibatide from nanocapsules by shear stress was 0.361 µM / 1.47 µM =24.6%.

Shear dependent inhibition of platelet aggregation *in vitro* by E-NCs

To assess the shear rate threshold for drug release, citrate anticoagulated whole blood in the presence of 1.23 mg/ml E-NCs ($2.8x10^{12}$ particles / ml) loaded with 350 µM eptifibatide was perfused over a matrix of 200 µg/ml collagen type I at 500 s^{-1}, 1,000 s^{-1} and 3,000 s^{-1} shear rate in conventional straight microfluidic channels (1mm (w) x 52µm (h)). Consistent with the stenosis channels, E-NCs did not affect total platelet aggregate volume at 500 s^{-1} and 1,000 s^{-1}. At 3,000 s^{-1} platelet aggregation was reduced in the presence of E-NCs (Fig. 2a,b). The shear dependency of the inhibition indicates that potential passive eptifibatide leakage prior to perfusion is minimal and is not affecting the capacity of the nanocapsules. To assess the exact shear rate at which the nanocapsules release their contents and inhibit thrombus formation we designed and employed a tapering microfluidic channel to produce a gradual increase from 300 s^{-1} at the inlet to 3,400 s^{-1} at the outlet as determined by computational fluidic dynamics modelling (Fig. 2c). The channel was coated with 50 µg/mL collagen type I and perfused with whole blood in the presence or absence of 1.23 mg/ml E-NCs ($2.8x10^{12}$ particles/ml) E-NCs. Under control conditions, platelet aggregate size shear dependently increased from ~1,000 s^{-1} onwards (Fig. 2d). Consistent with the results in Fig. 2a, platelet aggregate sizes in the presence of 350 µM E-NCs were not statistically different to control up to 1,000 s^{-1}. Statistical difference between PBS-NCs and E-NCs was reached at 2,200 s^{-1}. Nanocapsules loaded with 2 mM eptifibatide significantly reduced platelet aggregate size from 1,500 s^{-1} onwards. (Fig. 2d). These data demonstrate that release of encapsulated eptifibatide is shear rate dependent and sufficient to limit platelet aggregate formation at high shear rates.

To directly visualize the behaviour of the nanocapsules during their travel through the stenotic segment in the microfluidic channels we applied high-speed fluorescence microscopy. Nanocapsules were loaded with 20 µM 5(6)-carboxyfluorescein, perfused in

PBS through the stenosis channels at 1,000 s^{-1} input shear and imaged at 20,000 frames per second. Consistent with the light scattering results (supplementary fig 1), nanocapsules did not show visible signs of rupture or disintegration in the stenotic sections during perfusion (Suppl. Fig. 3a). However, there was a relative increase in the fluorescence intensity of the nanocapsules as they passed through the apex of the stenosis (Suppl. Fig. 3a). Importantly, the increase in nanocapsule fluorescence intensity in the apex of the stenosis was further increased when the nanocapsules were perfused in a medium with higher viscosity; 50% (v/v) plasma in PBS and 100% plasma (Suppl. Fig. 3b). These data indirectly demonstrate that stenotic segments expose nanocapsules to mechanical stressors that have viscosity (shear stress) dependent effects on the nanocapsules.

Nanocapsule release of eptifibatide is shear dependent.

To verify that the release of antiplatelet drugs from the NCs was driven by a shear dependent process we partially destabilized the lipid bilayer of the NCs with ethoxylated fatty alcohol poly(oxyethylene)(10) stearyl ether (Brij76). This detergent increases permeability of the PC membrane which aids shear induced pore formation and consequent drug release [15, 16]. Citrate anticoagulated whole blood in the presence of 1.23 mg/ml E-NCs ($2.8x10^{12}$ particles / ml) E-NCs loaded with 350 µM eptifibatide and containing 0.06mol% Brij76 was perfused over a matrix of collagen type I. Brij76 E-NCs did not affect total platelet surface area coverage at 500 s^{-1}. However, in contrast to E-NCs without detergent (fig. 2), platelet surface area was significantly reduced at 1,000 s^{-1} to the level of 1.4µM free eptifibatide (Fig. 3a,b). The incorporation of Brij76 reduced the shear threshold for drug release from >1,500s^{-1} as shown in Fig. 2d to between 500 s^{-1} and 1,000 s^{-1}.

To further characterize the shear dependent relationship between the nanocapsule stability and inhibition of platelet aggregation, Brij76 concentrations were varied from 0 to 0.12 mol% and tested at 500 s^{-1} and 1,000 s^{-1}. Progressive reduction of the nanocapsule stability with increasing Brij76 concentrations led to a concomitant reduction in platelet aggregate formation at 1,000 s^{-1} but not at 500s^{-1} (Fig. 3c). Nano capsule delivery of eptifibatide is shear dependent above a threshold that can be modulated through partial destabilization of the lipid bilayer with Brij76.

Antiplatelet nanocapsules prevent thrombotic occlusion *in vivo*.

To demonstrate the antithrombotic efficacy of the shear sensitive antiplatelet nanocapsules *in vivo* we assessed to effect of E-NCs loaded with 350 µM eptifibatide that were administrated

i.v. into C57/Bl6 mice (100 µl at 12.3 mg/ml corresponding to $2.8x10^{12}$ nanocapsules) 5 minutes prior to ferric chloride-induced carotid artery injury. Infusion of $2.8x10^{12}$ PBS-NCs resulted in similar occlusion times as compared to PBS vehicle only (Fig. 4a). To validate the shear sensitivity of the nanocapsules, intact E-NCs composed with and without 0.06% Brij76 were introduced in the carotid artery injury model. The presence of 0.06% Brij76 resulted in a loss of efficacy of the nanocapsules (Fig. 4b), likely due to shear disruption of the nanocapsules in the normal mouse circulation [17]. Stabilization of the nanocapsules by removal of Brij76 rescued the antithrombotic capacity of the E-NCs (Fig. 4b,c). Manual shear disruption of E-NCs prior to infusion resulted in a failure to maintain vessel patency with blood flow reducing to zero in 7-8 minutes, indicating that when eptifibatide is released prior to infusion, the final systemic concentrations of the drug remain below effective doses that prevent vessel occlusion. Extending the time from injection to vessel injury from 5 minutes to 40 minutes resulted in a loss of E-NC efficacy (Fig 4c). Consistent with this, E-NCs displayed a biphasic clearance with a half-life of 10 minutes (Fig. 4d). 2 hours following injection, the majority of E-NCs were localized to the spleen and liver (Fig. 4e).

Antiplatelet nanocapsules reduce pulmonary thrombus load

In mice, the venous circulation harbors on average ~4-fold lower shear stress levels compared to the arterial circulation [17], however since local shear stress levels during occlusive thrombus formation can increase up to 100-fold [18], shear sensitive nanocapsules may also inhibit occlusive thrombus formation in the venous circulation or reduce the impact of venous emboli in the high shear vascular system of the lungs. Thus we assessed the applicability of E-NCs in reducing thrombus formation that originated in the venous circulation. In contrast to traditional PE models where preformed emboli are injected, we measured the extent of thrombus load in the lung induced by i.v. injection of Innovin (containing tissue factor, phospholipids and calcium) in the tail vein in the presence of $2.8x10^{12}$ circulating E-NCs loaded with 350 µM eptifibatide. Fluorescently labeled fibrin(-ogen) was used to visualize and quantify emboli in the lungs. We first tested if a single high dose of free eptifibatide injected at the clinical loading dose of 180 µg/kg prior to the administration of Innovin could reduce the total load of emboli in the lung. Under control conditions, 12.5±1.7% of the total lung surface area was occupied by fibrin(-ogen) rich structures (Fig. 5a). A single dose of E-NCs reduced the fibrin(-ogen) content in the lungs to 3.8±0.4% (Fig.5a,b), which was similar to the fibrin(-ogen) content following administration of 180 µg/kg free eptifibatide. Although

no assessment can be made on the qualitative features of the fibrin rich structures, the total burden of fibrin deposition in the lungs was reduced in the presence of E-NCs.

Antiplatelet nanocapsules do not prolong tail bleeding time

To assess the haemostatic profile in the presence of E-NCs tail bleeding times were monitored. A longitudinal incision was made over the left peripheral tail vein 1 cm from the proximal end of the tail and time for cessation of bleeding to occur was monitored. Injection of PBS nanocapsules resulted in a baseline bleeding time of 200 seconds whereas injection of a clinical loading dose of free eptifibatide (180µg/kg) increased bleeding time to 800 seconds (Fig. 6). $2.8x10^{12}$ E-NCs loaded with 2 mM eptifibatide did not increase bleeding time compared to PBS-NCs. Similar, E-NCs that were manually shear disrupted prior to injection did not increase tail vein bleeding times. These data demonstrate that under these conditions the presence of shear sensitive antiplatelet nanocapsules do not lead to sufficiently high systemic drug concentrations that interfere with normal haemostasis and thereby prolong tail vein bleeding times.

Discussion

We previously demonstrated that stenotic sites are prothrombotic, particularly downstream of stenotic vessel segments due to large variations in shear stress [3, 4]. While mechanical forces play a well-recognized role in arterial thrombosis [1, 3], traditional antiplatelet therapies rely on chemically targeting platelet adhesion receptors and intracellular activation pathways. The link between pathological shear stress and exacerbated thrombus formation has justified recent developments of shear sensitive nanotherapeutics [9, 15, 19]. However, strategies to site specifically inhibit platelet adhesion by exploiting the shear stress at sites of occlusive thrombus formation have not been explored. The lack of suitable *in vitro* and *in vivo* thrombosis models has hampered the accurate assessment of targeted delivery of antiplatelet drugs. We have applied microfluidic- and mouse thrombosis models to test the hypothesis that membrane pore formation [20] and release of high dose antiplatelet drugs from nanocapsules occurs site specifically when local shear rate levels increase due to a thrombus developing to near occlusive dimensions. We encapsulated the antiplatelet agent eptifibatide (Integrilin) in shear sensitive nanocapsules composed of EggPC. Eptifibatide binds reversibly to GPIIb/IIIa and is only used in selected patients, typically undergoing high risk PCI, because of the associated risk of bleeding [21, 22]. Based on side effects of bleeding

the clinical use is restricted and has become less with the availability of oral $P2Y_{12}$ inhibitors [23]. We found that shear sensitive antiplatelet nanocapsules released eptifibatide sufficiently to limit platelet aggregate size and surface coverage *in vitro* and prevented thrombotic occlusion *in vivo* under conditions where blood shear rates reached pathological levels. The absence of nanocapsules inside a developing thrombus is consistent with other reports [24] and excluded the possibility that they became trapped and subsequently released drugs in a shear independent manner. Local shear rates of vessels constricted by thrombi, can increase one to two orders of magnitude [25] indicating that shear sensitive nanocapsules could be effective in both the arterial and venous circulation. Indeed, thrombi formed in the venous circulation in the presence of antiplatelet nanocapsules displayed less thrombus load in the lung circulation. Although the mechanisms of venous thrombus formation are distinct from arterial (mural) thrombus formation, a key role for pathologic high shear in both models is likely [9]. Tail bleeding times which represent a model for drug safety and an indication of haemostatic potential, not thrombotic potential, were normal in the presence of antiplatelet nanocapsules. The mechanism by which antiplatelet nanocapsules allow platelet plug formation during the tail bleeding assay, yet efficiently prevent thrombotic occlusion in the thrombosis models is beyond the scope of this study but likely involves a significant difference in local shear rates between these models. Indeed, thrombus formation in a vessel wall puncture with blood extravasation typically leads to a thrombus that grows intraluminal by no more than 50% [26] which is insufficient to significantly increase local shear rates.

Effective inhibition of occlusive thrombus formation by antiplatelet nanocapsules is directly determined by the amount of drug locally released from the nanocapsules. It proved unfeasible to determine release kinetics of eptifibatide at sites of developing thrombi. Thus, we monitored the functional consequence of local drug release: inhibition of thrombus formation. In our study systemic concentrations of eptifibatide remained very low. The injection of $2.8x10^{12}$ nanocapsules (10.53 µl internal volume) with encapsulated eptifibatide at 350 µM in mice with 2.0 mL blood bed volume would lead to a maximal systemic concentration of 0.453 µM. This value is based on the assumption that maximally 24.6% of encapsulated eptifibatide can be released in a shear dependent manner, as determined in fig. 1. Importantly, this brief systemic eptifibatide concentration is 5.9-fold lower than current clinical loading doses in patients (180 µg/kg; equating to 2.7 µM in the mouse). Despite these low systemic concentrations, the complete protection against vessel occlusion under the described conditions underscores the high efficiency of site specific drug release by antiplatelet nanocapsules.

Key limitations of these studies are that no viable endothelium was incorporated in the flow channels and abstract vessel geometries were used. Both features may have influenced the anti-platelet activity of the nanocapsules. The *in vivo* thrombosis models feature severe vessel damage by ferric chloride or strong initiators of coagulation which is non-physiological but nonetheless demonstrated the high efficacy of the eptifibatide nanocapsules.

While the shear sensitive nature of lipid vesicles has been described [27], this property has not been harnessed in the setting of antiplatelet therapy. We verified that the local delivery of antiplatelet drugs was a shear dependent process by altering the membrane composition with polyoxyethylene-10-stearyl ether (Brij76) which is known to destabilize the lipid membrane and consequently decrease the shear stress threshold for membrane pore formation [16]. This tuneability of shear stress sensitivity may prove to be beneficial when the antiplatelet nanocapsules are going to be investigated in larger animal models where the vascular bed operates at different shear stress levels [17].

The circulation half-life of PC-based liposomes is in the order of hours [28] which, in its present setup, makes this approach an ideal therapy option in the setting of acute coronary syndrome (ACS) and PCI where a rapidly reversible antiplatelet effect is highly desired [29, 30]. The short half-life of the antiplatelet nanocapsules may allow for a reversible and potent therapeutic window with lower bleeding risk because it only inhibits platelets if and where vessel occlusion would occur.

This study represents a step towards the clinical introduction of nanoparticle based treatment of thrombotic complications such as in the setting of acute coronary syndrome that may be more potent and safer than existing therapies.

Acknowledgements

This work was supported by grants from the National Health and Medical Research Council Australia (NHMRC; 1083138 and 1050018) and Perpetual grants Australia (FR2014/0941). CEH and EW were supported by the National Heart Foundation (CR 11M 6066, 100123). AJM is supported by a career development fellowship from the NHMRC (APP1085752) and a future leader fellowship from the National Heart Foundation (100440). KP is supported by an NHMRC fellowship (1079492). We thank Irene Ung for technical assistance with the in vitro blood perfusion experiments. The authors gratefully acknowledge the contribution toward this study from the Victorian Operational Infrastructure Support Program.

Author contributions

C. Molloy performed experiments, analyzed and interpreted data; J. Yao performed experiments, analyzed and interpreted data; H. Kammoun performed experiments, analyzed and interpreted data; T. Bonnard performed experiments, analyzed and interpreted data; T. Hoefer analyzed and interpreted data; K. Alt performed experiments, analyzed and interpreted data; F. Tovar-Lopez performed CFD analysis and compiled figures; G. Rosengarten provided essential tools, analyzed and interpreted data; P. Ramsland provided essential tools, performed experiments and analysed and interpreted data; A. van der Meer provided essential tools, analyzed and interpreted data; A.van de Berg provided essential tools, analyzed and interpreted data; A. Murphy analyzed and interpreted data; C. Hagemeyer analyzed and interpreted data; K. Peter designed research, analyzed and interpreted data; E. Westein designed research, performed experiments, analyzed and interpreted data. All authors contributed to paper writing and manuscript revision

Disclosure

A. Van der Meer reports personal fees from Emulate, Inc. outside the submitted work; In addition, A. Van der Meer has a pending patent on "Methods, Systems, And Compositions For Determining Platelet Function, And Uses Thereof"

Other authors have nothing to disclose.

Supporting Information

Supplementary figures S1-S3

References

1 Ruggeri ZM, Orje JN, Habermann R, Federici AB, Reininger AJ. Activation-independent platelet adhesion and aggregation under elevated shear stress. *Blood*. 2006.

2 Colace TV, Diamond SL. Direct observation of von Willebrand factor elongation and fiber formation on collagen during acute whole blood exposure to pathological flow. *Arteriosclerosis, thrombosis, and vascular biology*. 2013; **33**: 105-13. 10.1161/ATVBAHA.112.300522.

3 Westein E, van der Meer AD, Kuijpers MJ, Frimat JP, van den Berg A, Heemskerk JW. Atherosclerotic geometries exacerbate pathological thrombus formation poststenosis in a von Willebrand factor-dependent manner. *Proceedings of the National Academy of Sciences of the United States of America*. 2013; **110**: 1357-62. 10.1073/pnas.1209905110.

4 Nesbitt WS, Westein E, Tovar-Lopez FJ, Tolouei E, Mitchell A, Fu J, Carberry J, Fouras A, Jackson SP. A shear gradient-dependent platelet aggregation mechanism drives thrombus formation. *Nature medicine*. 2009; **15**: 665-73. nm.1955 [pii] 10.1038/nm.1955.

5 Barstad RM, Orvim U, Hamers MJ, Tjonnfjord GE, Brosstad FR, Sakariassen KS. Reduced effect of aspirin on thrombus formation at high shear and disturbed laminar blood flow. *Thrombosis and haemostasis*. 1996; **75**: 827-32.

6 Stoll P, Bassler N, Hagemeyer CE, Eisenhardt SU, Chen YC, Schmidt R, Schwarz M, Ahrens I, Katagiri Y, Pannen B, Bode C, Peter K. Targeting ligand-induced binding sites on GPIIb/IIIa via single-chain antibody allows effective anticoagulation without bleeding time prolongation. *Arteriosclerosis, thrombosis, and vascular biology*. 2007; **27**: 1206-12. 10.1161/ATVBAHA.106.138875.

7 Wang X, Palasubramaniam J, Gkanatsas Y, Hohmann JD, Westein E, Kanojia R, Alt K, Huang D, Jia F, Ahrens I, Medcalf RL, Peter K, Hagemeyer CE. Towards Effective and Safe Thrombolysis and Thromboprophylaxis: Preclinical Testing of a Novel Antibody-Targeted Recombinant Plasminogen Activator Directed Against Activated Platelets. *Circulation research*. 2014; **114**: 1083-93. 10.1161/CIRCRESAHA.114.302514.

8 Hohmann JD, Wang X, Krajewski S, Selan C, Haller CA, Straub A, Chaikof EL, Nandurkar HH, Hagemeyer CE, Peter K. Delayed targeting of CD39 to activated platelet GPIIb/IIIa via a single-chain antibody: breaking the link between antithrombotic potency and bleeding? *Blood*. 2013; **121**: 3067-75. 10.1182/blood-2012-08-449694.

9 Korin N, Kanapathipillai M, Matthews BD, Crescente M, Brill A, Mammoto T, Ghosh K, Jurek S, Bencherif SA, Bhatta D, Coskun AU, Feldman CL, Wagner DD, Ingber DE. Shear-activated nanotherapeutics for drug targeting to obstructed blood vessels. *Science*. 2012; **337**: 738-42. 10.1126/science.1217815.

10 Andresen TL, Jensen SS, Jorgensen K. Advanced strategies in liposomal cancer therapy: problems and prospects of active and tumor specific drug release. *Progress in lipid research*. 2005; **44**: 68-97. 10.1016/j.plipres.2004.12.001.

11 Murday JS, Siegel RW, Stein J, Wright JF. Translational nanomedicine: status assessment and opportunities. *Nanomedicine : nanotechnology, biology, and medicine*. 2009; **5**: 251-73. 10.1016/j.nano.2009.06.001.

12 Weller GH, Tabor G, Jasak H, Fureby C. A tensorial approach to computational continuum mechanics using object-oriented techniques. *Computer in Physics*, 1998.

13 Tovar-Lopez FJ, Rosengarten G, Khoshmanesh K, Westein E, Jackson SP, Nesbitt WS, Mitchell A. Structural and hydrodynamic simulation of an acute stenosis-dependent thrombosis model in mice. *J Biomech*. 2011; **44**: 1031-9. 10.1016/j.jbiomech.2011.02.006.

14 Tovar-Lopez FJ, Rosengarten G, Nasabi M, Sivan V, Khoshmanesh K, Jackson SP, Mitchell A, Nesbitt WS. An investigation on platelet transport during thrombus formation at micro-scale stenosis. *PloS one*. 2013; **8**: e74123. 10.1371/journal.pone.0074123.

15 Holme MN, Fedotenko IA, Abegg D, Althaus J, Babel L, Favarger F, Reiter R, Tanasescu R, Zaffalon PL, Ziegler A, Muller B, Saxer T, Zumbuehl A. Shear-stress sensitive lenticular vesicles for targeted drug delivery. *Nature nanotechnology*. 2012; **7**: 536-43. 10.1038/nnano.2012.84.

16 Bernard AL, Guedeau-Boudeville MA, Marchi-Artzner V, Gulik-Krzywicki T, di Meglio JM, Jullien L. Shear-induced permeation and fusion of lipid vesicles. *J Colloid Interface Sci*. 2005; **287**: 298-306. 10.1016/j.jcis.2004.12.019.

17 Cheng C, Helderman F, Tempel D, Segers D, Hierck B, Poelmann R, van Tol A, Duncker DJ, Robbers-Visser D, Ursem NT, van Haperen R, Wentzel JJ, Gijsen F, van der Steen AF, de Crom R, Krams R. Large variations in absolute wall shear stress levels within one species and between species. *Atherosclerosis*. 2007; **195**: 225-35. 10.1016/j.atherosclerosis.2006.11.019.

18 Bark DL, Jr., Ku DN. Wall shear over high degree stenoses pertinent to atherothrombosis. *J Biomech*. 2010; **43**: 2970-7. S0021-9290(10)00392-1 [pii]
10.1016/j.jbiomech.2010.07.011.

19 Greineder CF, Howard MD, Carnemolla R, Cines DB, Muzykantov VR. Advanced drug delivery systems for antithrombotic agents. *Blood*. 2013; **122**: 1565-75. 10.1182/blood-2013-03-453498.

20 Sandre O, Moreaux L, Brochard-Wyart F. Dynamics of transient pores in stretched vesicles. *Proceedings of the National Academy of Sciences of the United States of America*. 1999; **96**: 10591-6.

21 Chan AW, Moliterno DJ, Berger PB, Stone GW, DiBattiste PM, Yakubov SL, Sapp SK, Wolski K, Bhatt DL, Topol EJ, Investigators T. Triple antiplatelet therapy during percutaneous coronary intervention is associated with improved outcomes including one-year survival: results from the Do Tirofiban and ReoProGive Similar Efficacy Outcome Trial (TARGET). *Journal of the American College of Cardiology*. 2003; **42**: 1188-95.

22 Bhatt DL, Lincoff AM, Gibson CM, Stone GW, McNulty S, Montalescot G, Kleiman NS, Goodman SG, White HD, Mahaffey KW, Pollack CV, Jr., Manoukian SV, Widimsky P, Chew DP, Cura F, Manukov I, Tousek F, Jafar MZ, Arneja J, Skerjanec S, Harrington RA, Investigators CP. Intravenous platelet blockade with cangrelor during PCI. *The New England journal of medicine*. 2009; **361**: 2330-41. 10.1056/NEJMoa0908629.

23 Bassler N, Loeffler C, Mangin P, Yuan Y, Schwarz M, Hagemeyer CE, Eisenhardt SU, Ahrens I, Bode C, Jackson SP, Peter K. A mechanistic model for paradoxical platelet activation by ligand-mimetic alphaIIb beta3 (GPIIb/IIIa) antagonists. *Arteriosclerosis, thrombosis, and vascular biology*. 2007; **27**: e9-15. 10.1161/01.ATV.0000255307.65939.59.

24 Heger M, Salles, II, van Vuure W, Hamelers IH, de Kroon AI, Deckmyn H, Beek JF. On the interaction of fluorophore-encapsulating PEGylated lecithin liposomes with hamster and human platelets. *Microvascular research*. 2009; **78**: 57-66. 10.1016/j.mvr.2009.02.006.

25 Wootton DM, Ku DN. Fluid mechanics of vascular systems, diseases, and thrombosis. *Annu Rev Biomed Eng*. 1999; **1**: 299-329. 1/1/299 [pii]
10.1146/annurev.bioeng.1.1.299.

26 oude Egbrink MG, Tangelder GJ, Slaaf DW, Reneman RS. Thromboembolic reaction following wall puncture in arterioles and venules of the rabbit mesentery. *Thrombosis and haemostasis*. 1988; **59**: 23-8.

27 Noguchi H, Gompper G. Fluid vesicles with viscous membranes in shear flow. *Physical review letters*. 2004; **93**: 258102.

28 Senior J, Crawley JC, Gregoriadis G. Tissue distribution of liposomes exhibiting long half-lives in the circulation after intravenous injection. *Biochimica et biophysica acta*. 1985; **839**: 1-8.

29 Marosfoi MG, Korin N, Gounis MJ, Uzun O, Vedantham S, Langan ET, Papa AL, Brooks OW, Johnson C, Puri AS, Bhatta D, Kanapathipillai M, Bronstein BR, Chueh JY, Ingber DE, Wakhloo AK. Shear-Activated Nanoparticle Aggregates Combined With Temporary Endovascular Bypass to Treat Large Vessel Occlusion. *Stroke*. 2015; **46**: 3507-13. 10.1161/STROKEAHA.115.011063.

30 Korin N, Gounis MJ, Wakhloo AK, Ingber DE. Targeted drug delivery to flow-obstructed blood vessels using mechanically activated nanotherapeutics. *JAMA neurology*. 2015; **72**: 119-22. 10.1001/jamaneurol.2014.2886.

Figure legends

Figure 1. Antiplatelet nanocapsules target thrombi in stenotic vessel segments. a) Schematic of the *in vitro* microfluidic channels used, incorporating a semicircular sidewall protrusion of 80% to induce a shear rate in the apex that is 8-fold higher than the input shear rate. **b**) Citrate anticoagulated whole blood, labelled with 0.5 µg/mL DiOC6 and loaded with either PBS nanocapsules (PBS-NCs) or eptifibatide nanocapsules (E-NCs) was perfused at 1,000 s^{-1} input shear rates and imaged upstream and inside the stenosis. Images show false colour staining of platelet aggregates after 5 min perfusion. Scale bar, 100 µm. **c**) Platelet aggregate surface area in the presence of PBS, PBS-NCs, E-NCs or free eptifibatide at the upstream and stenotic sections of the channel where shear rates are 1,000 s^{-1} and 8,000 s^{-1} respectively. Data are mean+s.e.m., n=4. *P<0.05. **d)** Differential interference contrast (i) and fluorescent images (ii) of DiOC6 labelled platelet thrombi (red) on collagen type I following blood perfusion in the presence of NBD-PE labelled NCs (green). (iii) Long exposure fluorescent snapshot (200ms) of NBD-PE-NCs during blood perfusion. The streaks indicate that NCs are free flowing and not being incorporated into thrombi. Scale bar, 20 µm. **e**) Maximum ADP-induced platelet aggregation expressed as % light transmission. Human PRP

(230 µl) was incubated with $2.8x10^{11}$ E-NCs (10 µl) that were intact or shear disrupted. Platelet aggregation was initiated by 5 µM ADP (10 µl). PBS and free eptifibatide (1.4 µM) were used as positive and negative control respectively. Data are mean+s.e.m., n=3. ***P<0.001, ****P<0.0001. **f**) Maximum aggregation levels of PRP induced by 5 µm ADP in the presence of indicated concentrations of free eptifibatide. Data are mean+s.e.m., n=4.

Figure 2. Drug release from antiplatelet nanocapsules is shear rate dependent. a) Representative micrographs showing adhesion of DiOC6-labelled platelets after perfusion of whole blood in the presence of PBS, PBS-NCs, E-NCs or free eptifibatide (1.4 µM) over a 200 µg/ml collagen type I matrix at 500, 1,000 and 3,000 s^{-1} shear rate. Scale bar, 50 µm. **b**) Surface area coverage of platelet aggregates displayed in a). E-NCs were resistant to drug release at 500 and 1,000 s^{-1} but not at 3,000 s^{-1}. Data are mean+s.e.m., n=3-6. ****P<0.0001. **c**) A tapering microfluidic channel with dimensions from 1,000x52 µm to 100x52 µm over a distance of 16 mm was coated with 50 µg/mL collagen type I and perfused at an entrance shear of 300 s^{-1} with whole blood in the presence of E-NCs. CFD analysis demonstrates a gradual increase from 300 s^{-1} at the inlet to 3,400 s^{-1} at the outlet. **d**) Average platelet aggregate size as function of position in the tapering channel, expressed as governing shear rate. Whole blood was perfused in the presence of nanocapsules loaded with PBS or eptifibatide encapsulated at 350 µM or 2 mM. Data are mean+s.e.m., n=3 *p<0.05 (Multiple t-tests).

Figure 3. Shear threshold for nanocapsule drug release can be modulated with Brij76.
a) Representative micrographs showing adhesion of DiOC6-labelled platelets to collagen type I (200 µg/mL) after 5 minutes perfusion of citrate (3.2%) anticoagulated whole blood through microfluidic channels at shear rates of 500 s^{-1} or 1,000 s^{-1} in the presence of PBS-NCs or E-NCs loaded with 350 µM eptifibatide or free eptifibatide (1.4 µM). The nanocapsules were supplemented with 0.06mol% Brij76 to shear sensitize the lipid membrane resulting in an inhibitory effect at 1,000 s^{-1} but not at 500 s^{-1}. Scale bar, 100 µm. **b**) Mean surface area coverage of platelets displayed in a). Data are mean+s.e.m., n=4. **c**) E-NCs with varying Brij76 concentrations were added to whole blood and perfused over a collagen type I matrix at 500 s^{-1} (○) or 1,000 s^{-1} (●) shear rate. Platelet aggregate surface coverage was monitored as function of Brij76 content in the E-NCs and normalized against the surface coverage at 0mol% Brij76. Data are mean+s.e.m. n=5. *P<0.05, ***P<0.001, ****P<0.0001.

Figure 4. Antiplatelet nanocapsules prevent arterial thrombosis. **a**) Blood flow in a mouse carotid artery after vessel injury induced by 5% $FeCl_3$ and infusion with $2.8x10^{12}$ (100 µl) shear disrupted PBS-NCs (●) or no treatment (○). Data are mean+s.e.m., n=4. **b**) Blood flow in a mouse carotid artery after vessel injury induced by 5% $FeCl_3$ and infusion with $2.8x10^{12}$ (100 µl) intact E-NCs in the presence (●) or absence (●) of 0.06mol% Brij76, or shear disrupted E-NCs (□). Data are mean+s.e.m., n=3-6. **c**) Carotid artery patency times of indicated E-NCs. Intact PBS-NCs served as control. ****P<0.0001. **d)** Blood clearance of NDB labelled E-NCs, normalized against injection dose. Data are mean+s.e.m. n=3. **e)** Organ biodistribution of E-NCs containing trace amounts of ^{3}H-[PC]. Graph depicts liquid scintillation counts per milligram of tissue. Quad, quadriceps muscle; WAT, white adipose tissue. Data are mean+s.e.m. n=4.

Figure 5. E-NCs reduce pulmonary thrombus load. a) Fluorescent micrographs showing emboli in lungs of mice that were infused with a 100 µl mixture of Innovin (recombinant tissue factor and phospholipids) and Cy7-labelled fibrinogen following the injection of $2.8x10^{12}$ PBS-NCs (i), $2.8x10^{12}$ E-NCs loaded with 350 µM eptifibatide (ii) or 180 µg/kg free eptifibatide (iii). **b**) Mean relative content of fibrin(-ogen) staining expressed as percentage of total lung area. ***P<0.001, ****P<0.0001.

Figure 6. Tail bleeding is not affected by antiplatelet nanocapsules. Template tail bleeding times in mice infused with nanocapsules loaded with PBS-NCs, intact or shear disrupted E-NCs (2 mM encapsulated eptifibatide) or free eptifibatide (180 µg/kg bodyweight). Data are mean+s.e.m., n=4. ***P<0.001.

Supplementary Figure 1. Structural stability of flow sensitive nanocapsules. a,b) Dynamic light scattering was used to determine the nano particle size distribution before (black solid) and after (red) 10 passes through the microfluidic stenosis channel, described in fig 3a, at 5,000 s^{-1} input wall shear rate. Vortexing the nanoparticle sample for 3 minutes did not affect mean particle size (blue) whereas Triton X100 dispersed the lipid nanocapsules into micelles or small vesicles with a mean size of 35 nm (dashed line). Data are mean+s.e.m., n=3. ****P<0.0001. **c)** Size, polydispersity index and zeta potential for the E-NC nanocapsule suspension measured at 25°C and 37°C.

Supplementary Figure 2. Loading efficiency and release of eptifibatide from nanocapsules. Maximum ADP induced platelet aggregation expressed as light transmission. Human PRP (230 µl) was incubated with $2.8x10^{11}$ eptifibatide nanocapsules (10 µl) that were intact or shear disrupted. PBS-NCs and free eptifibatide (1.4 µM) were used as positive and negative control respectively. Platelet aggregation was initiated with 2.5 and 10 µM ADP (10 µl). Data are mean+s.e.m., n=3. ***P<0.001, ****P<0.0001.

Supplementary Figure 3 Microscopic assessment of individual nanocapsules during passage through a stenotic channel segment at 1,000 s^{-1} input shear rate. a) Carboxyfluorescein loaded nanocapsules were imaged in the stenosis inlet, apex and outlet with an exposure time of 50 µsec. A Gaussian blur (1 pixel radius) and false colour LUT was applied to visualize to apparent size increase in the stenosis apex compared to the inlet and outlet. **b)** Nanocapsules size increase, normalized against values obtained for nanocapsules in the inlet in PBS medium. Nanoparticle size was assessed in media with increasing viscosity: PBS, 1:1 diluted human plasma (50% P) and undiluted plasma (100% P). Median + interquartile range of 1 representative experiment with 800-3,000 nanocapsules interrogated. ****P<0.0001.

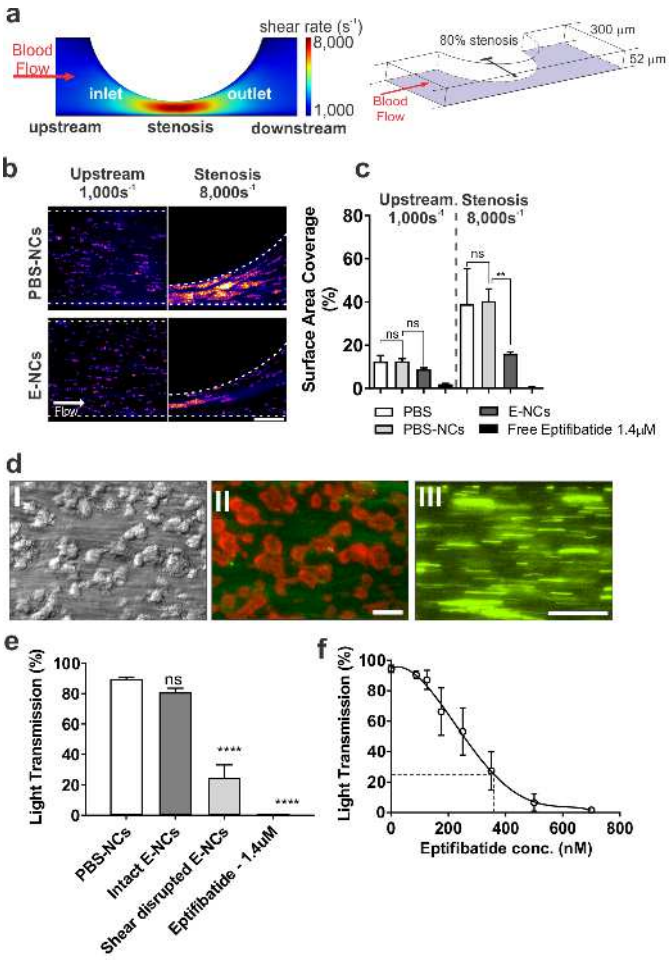

jth_13666_f1.tif

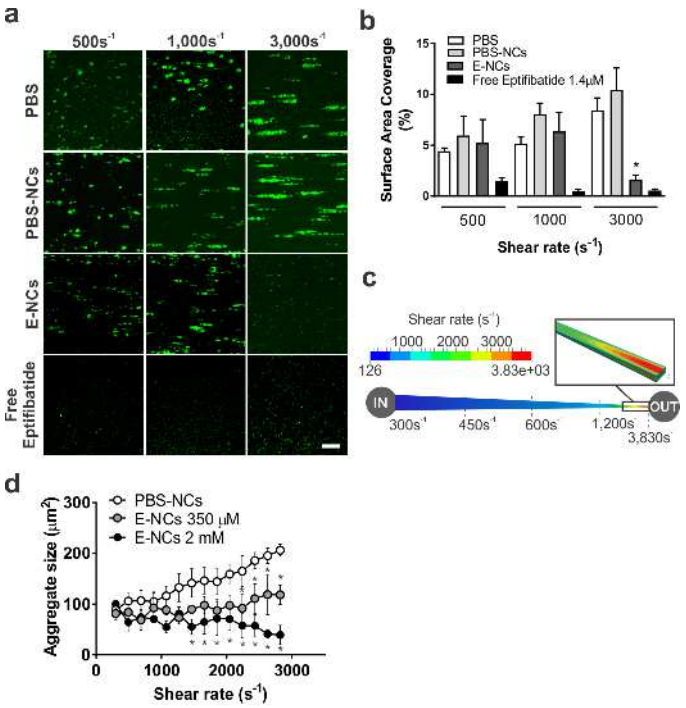

jth_13666_f2.tif

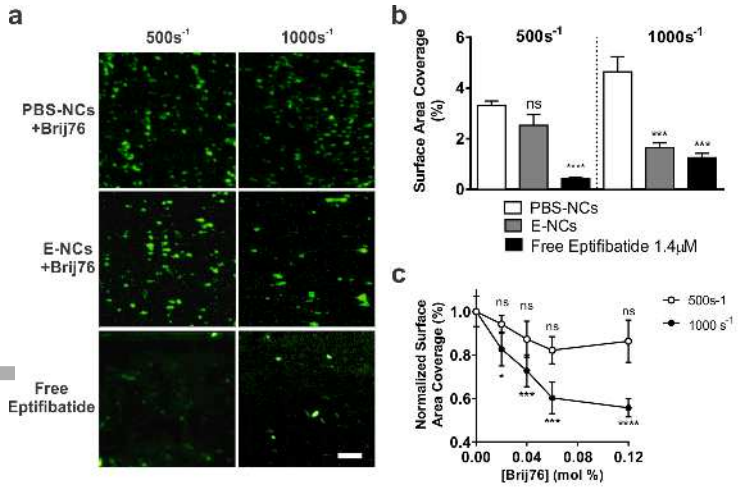

jth_13666_f3.tif

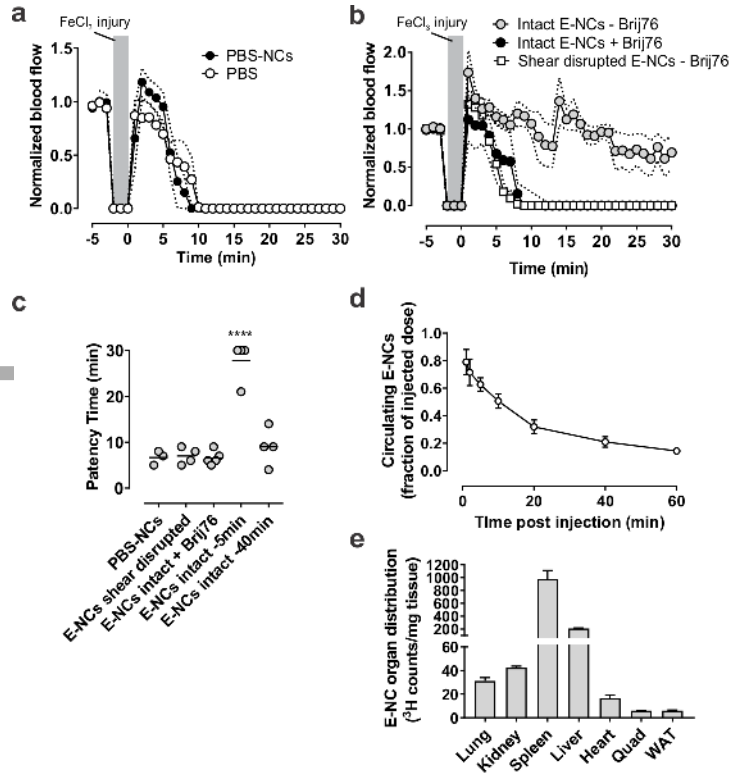

jth_13666_f4.tif

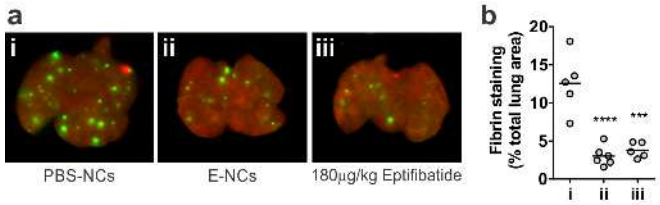

jth_13666_f5.tif

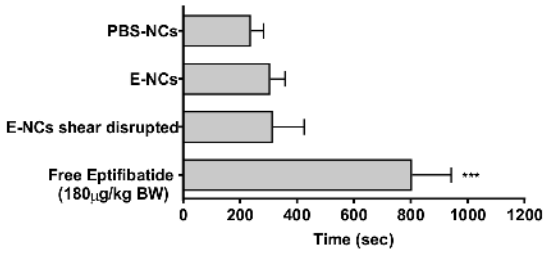

jth_13666_f6.tif